

University of Groningen

## Process of preparation and properties of ultra-high strength polyethylene fibers

Pennings, A.J.; Smook, J.; de Boer, J.; Gogolewski, S.; van Hutten, P.F.

*Published in:*  
Pure and Applied Chemistry

**IMPORTANT NOTE: You are advised to consult the publisher's version (publisher's PDF) if you wish to cite from it. Please check the document version below.**

*Document Version*  
Publisher's PDF, also known as Version of record

*Publication date:*  
1983

[Link to publication in University of Groningen/UMCG research database](#)

*Citation for published version (APA):*

Pennings, A. J., Smook, J., de Boer, J., Gogolewski, S., & van Hutten, P. F. (1983). Process of preparation and properties of ultra-high strength polyethylene fibers. *Pure and Applied Chemistry*, 55(5), 777-798.

### Copyright

Other than for strictly personal use, it is not permitted to download or to forward/distribute the text or part of it without the consent of the author(s) and/or copyright holder(s), unless the work is under an open content license (like Creative Commons).

The publication may also be distributed here under the terms of Article 25fa of the Dutch Copyright Act, indicated by the "Taverne" license. More information can be found on the University of Groningen website: <https://www.rug.nl/library/open-access/self-archiving-pure/taverne-amendment>.

### Take-down policy

If you believe that this document breaches copyright please contact us providing details, and we will remove access to the work immediately and investigate your claim.

*Downloaded from the University of Groningen/UMCG research database (Pure): <http://www.rug.nl/research/portal>. For technical reasons the number of authors shown on this cover page is limited to 10 maximum.*

## PROCESS OF PREPARATION AND PROPERTIES OF ULTRA-HIGH STRENGTH POLYETHYLENE FIBERS

A.J. Pennings, J. Smook, J. de Boer, S. Gogolewski and P.F. van Hutten.

Department of Polymer Chemistry, State University of Groningen, Nijenborgh 16,  
9747 AG Groningen, The Netherlands.

**Abstract-** High molecular weight polyethylene can be processed into fibers with tensile strengths at break of about 5 GPa and Young's moduli upto 200 GPa by either applying the "surface growth" technique or a combination of gel-spinning and hot-drawing. The mechanism of the molecular process in both techniques involves the oriented crystallization by stretching of an entanglement network. The high strength levels are only achieved either by crystallizing the stretched network or by drawing the semi-crystalline gel at relatively high temperatures in order to transform the elastically ineffective chain ends of the entanglement network into the strong backbone structure. Evidence is presented for the presence of entanglements in the ultra-strong polyethylene fibers and for the necessity of entanglement in achieving high strengths by hot-drawing. High fiber production rates of the order of 270 m/min. can be attained by adding 1 wt.% of aluminium stearate to the paraffin oil solution. This additive avoids the adsorption of polyethylene on the wall of the die and suppresses melt-fracture during extrusion.

### INTRODUCTION

It was not until relatively recently that a variety of routes were discovered, enabling to produce polymers with ultra-high modulus and strength. Mechanical properties comparable to those of metals have been achieved by hydrostatic extrusion of semi-crystalline polymers, also in combination with drawing (1-3), by hot-drawing under specific conditions of draw-rate and temperature (4-6), solidification of liquid-crystalline polymers, (7-9,24), solid-state polymerization of monomeric single crystals (10,11), simultaneous crystallization and polymerization of monomers (12), by zone-annealing (13) and oriented crystallization of entanglement networks (14-16) and hot-drawing of gels (17-20). The latter two techniques have been applied to linear polyethylene of very high molecular weight and tensile strengths of the fibers produced accordingly, have been attained as high as 5 GPa and Young's moduli upto 200 GPa.

Tensile properties at this level, aroused the interest of polymer scientists to investigate the morphology and texture of these fibers as well as the molecular mechanism associated with the oriented crystallization and deformation process. They also stimulated interest in exploring new applications in particular because these crystalline polymeric fibers possess relatively low densities and as a result of that their specific mechanical properties exceed those of steel and glass as is illustrated in Fig. 1. Technologists have need of stronger and lighter materials for the construction of aeroplanes and other means of transportation while these ultra-high strength fibers are also being looked for by designers of flywheels (21) for energy storage and of ultracentrifuges. Other areas of applications are e.g. microsurgery where the superstrong polyethylene fibers have successfully been employed as suture material for cornea transplantations and also for connecting tendons to bone. It is clear that one may conceive of several other new applications and its range will undoubtedly be broadened if the properties of the fibers will be varied by e.g. chemical modification. The purpose of the present paper is to give a brief account of various aspects of the process of preparation and of some mechanical properties of these polyethylene fibers. Therefore it is concerned with essential features of the "surface-growth" technique (16) and gel-spinning and hot-drawing (22,23). Both methods produce fibers with similar structure and properties. Additionally, we describe morphological observations which shed some light on the mechanism underlying the orientation and alignment of very long chain molecules in some stages of fiber formation. Originally the objective of this study was to grow better crystals by starting with very high molecular weight polyethylene thereby minimizing the defect concentration due to chain ends. This reduction in chain interruptions would obviously also increase the strength (25). But the processing of very large chain molecules entails the

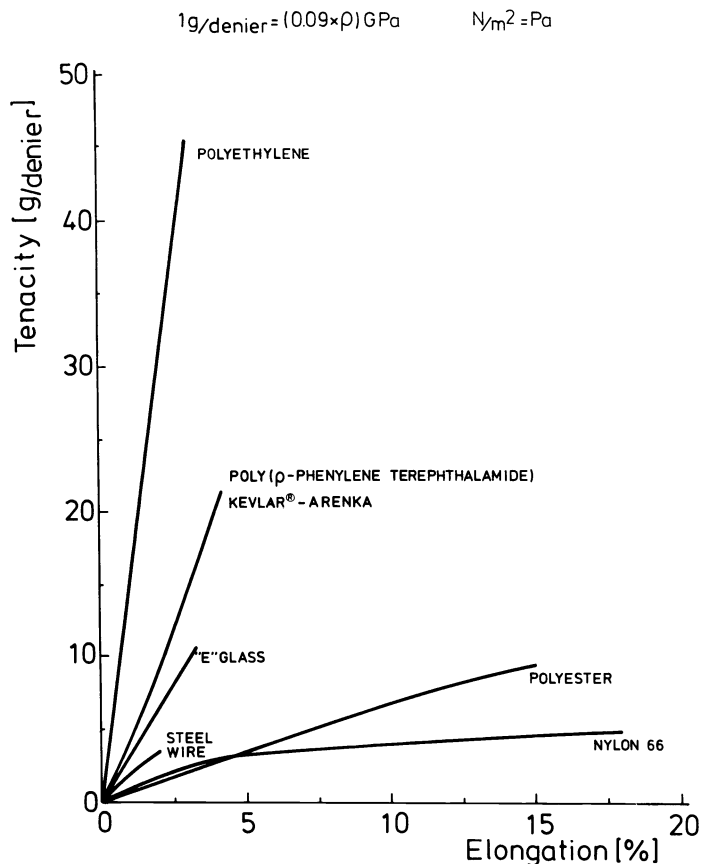


Fig. 1. Stress-strain behaviour of ultra-oriented polyethylene macrofibers compared with poly(p-phenylene terephthalamide), steel, glass, polyester and nylon.

probability of trapping topological defects (28) such as entanglement couplings of various degrees of complexity and twists and other disclinations (29,30) in addition to dislocations such as folds, Pechhold kinks (26), jogs (31) and Reneker point defects (27). Another cause of structural irregularities is due to the elastic properties of these long chains, giving rise to anomalous flow behaviour such as spiral flow, die swell and elastic turbulence (34-38). Entanglements seem to dominate the process and the fiber formation essentially amounts to stretching an entanglement network resulting in oriented crystallization as in schematically depicted in Fig. 3. Depending on the deformation rate,  $\dot{\epsilon}$ , the strands between entanglement couplings may be elastically active and are therefore liable to be transferred into a fibrous crystal. This only occurs if the orienting action of the flow field prevails over relaxation phenomena due to e.g. Brownian motion (39,40). The chain portions that are only on one end connected to the transient network will remain as cilia or dangling ends emerging from disordered domains which also contain trapped entanglements (28) and twist disclinations. These cilia may later crystallize epitaxially as chain-folded lamellae on the crystalline blocks of the backbones thereby generating the shish-kebab morphology. This morphological structure so characteristic for stirred solution crystallization (81), shows up as the main polyethylene crystal habit in the "surface growth" technique and also emerges as an intermediate in the gel-spinning and hot-drawing process.

In order to get a better understanding of the hot-drawing we have measured elongational viscosities and determined activation energies which give some idea of the molecular rearrangement and size of the flow units. Since the entanglements turned out to be so prevailing we have collected further evidence in the last but one section. Finally some mechanical properties are discussed and it will be shown that the fiber tensile strength depends rather strongly on the fiber diameter suggesting that surface flaws are responsible for early fracture.

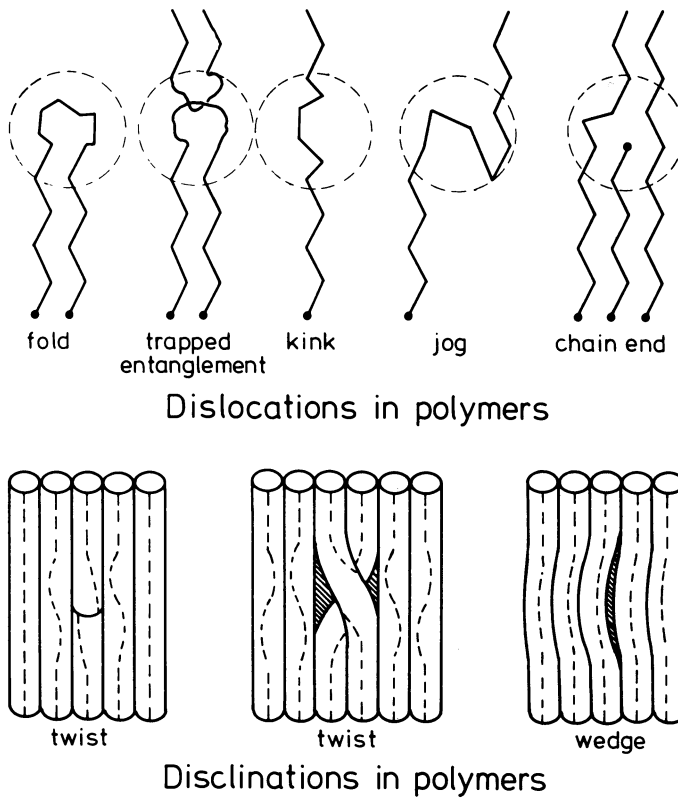


Fig. 2. Schematic representation of the main dislocations such as folds, kinks, jogs, trapped entanglements and disclinations such as twists in polymer crystals.

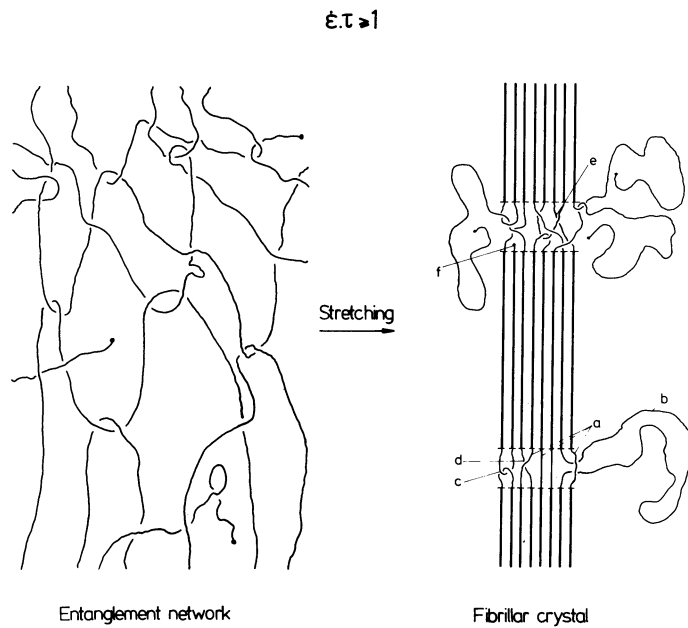


Fig. 3. Model showing the transformation of the entanglement network into highly oriented fibrillar crystallites. This transformation will only proceed successfully if the product of deformation rate  $\dot{\epsilon}$  and relaxation time for recoiling of the molecules  $\tau$  exceeds 1.

## PROCESS OF PREPARATION

## The "surface-growth" technique.

Superstrong polyethylene fibers can be produced in a one-step process which essentially consists of oriented crystallization due to stretching entangled high-molecular weight polymer molecules by subjecting dilute solutions to Couette flow while the growing fibrous crystal is being pulled out of the system (14-16,50). The experimental set-up of this technique as developed by Zwijnenburg (15) in our laboratory, schematically represented in Fig. 4, encompasses a beaker usually containing dilute supercooled solutions of polyethylene in p-xylene, a cylindrical rotor made of teflon, a take-up roll and a strain gage to measure the tension in the growing fiber. The general procedure of preparing these strong fibers is as

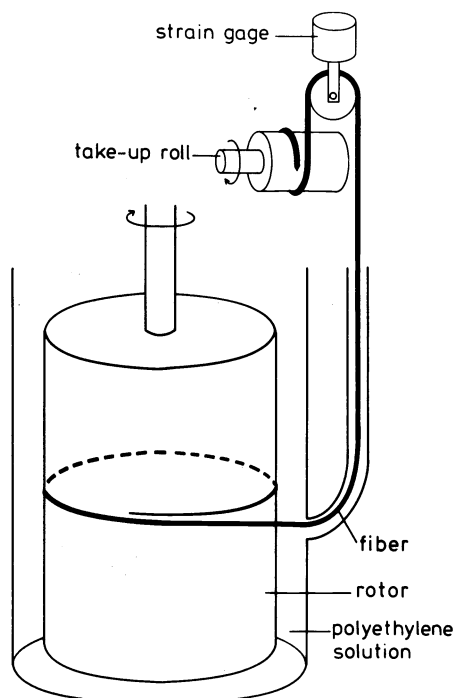


Fig. 4. Illustration of a Couette apparatus in which a polyethylene fiber is grown on the surface of a vertical rotor. The rotor is submerged in a polyethylene solution.

follows. After dissolution of the polyethylene at 130°C the solution is cooled down to e.g. 110°C in the case of p-xylene as a solvent and the rotor is set in motion. Subsequently a fibrous seed crystal is pushed through a small pipe attached to the beaker and is submerged in the solution. It will be aligned by the flowing solution and transported towards the rotor surface by following the streamlines. Once it comes into contact with the rotor surface the seed crystal starts to grow after some induction period, thereby pulling the rope, to which the seed is connected, taut. At that moment the take-up roll motor is switched on and its speed is adjusted in such a manner that it is equal to the longitudinal growth rate of the fibrous crystal. Once this steady state has been attained growth can be continued for many days.

Investigations of the influence of the roughness of the rotor surface and rotor material as well as of the solvent quality on the growth process (15,16) revealed that indeed adsorption of the very large polyethylene molecules plays an essential role. In fact, the fibrous crystal grows in a gel layer which adheres to the rotor surface. This could be clearly established by modifying the Couette-apparatus in such a way that the inner cylinder could rotate around a horizontal axis (41). By submerging it for only 1/3 in the polyethylene solution we could observe that the fiber did indeed grow all around the rotor in the gellayer still adhering to the rotor surface when it was above the solution level. Barham, Hill and Keller (42) provided further evidence for the existence of a gellayer and for the fact that this network is a prerequisite for fibrous growth by examining fiber growth boundaries and the occurrence of the gel as a function of temperature.

Basically, the adsorption of the very high molecular weight polyethylene on the rotor surface and the formation of the gellayer were already found to be a necessity for the nucleation of fibrous crystals in stirred solution crystallization experiments (43). Torfs (16) observed that in the "surface-growth" process, the fiber slides through the adsorbed gellayer and

growth appears to take primarily place at the lateral sides of the ribbon like fiber as is illustrated schematically in Fig. 5. Since adsorption of the very large molecules on the

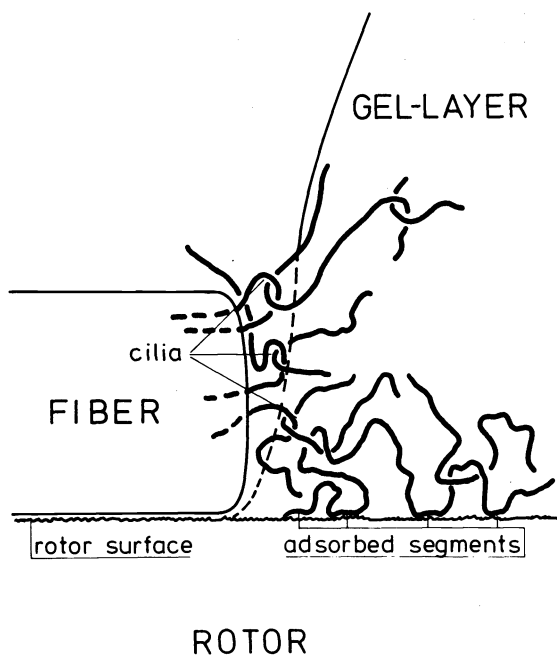


Fig. 5. Schematic drawing of a growing fiber in contact with molecules near the rotor surface. Trains of adsorbed segments are responsible for the adherence of molecules to the rotor surface. A gellayer is formed by entanglement connections between subsequent layers of molecules with the first adsorbed monolayer. This gellayer is additionally connected to the cilia exerting from the growing fiber through entanglements. The fiber and the adsorbed molecules on the rotor surface move in opposite directions, perpendicular to the plane of the paper.

rotor surface seems to play such a dominant role, it is pertinent for our understanding of the "surface-growth" process to look into the mechanism of adsorption in more detail. The conformation in the adsorbed state may be visualized by the generally accepted tail-train-loop model. Polymer molecules adhere to solid surfaces by multiple points of physical adsorption, which are interspaced with loops of long chain segments extending into the surrounding solution. The residence-time of a molecule on the surface increases with molecular weight and depends on the force of interaction between chain segment and surface molecules. It is to be expected that the residence-time also increases with the degree of supercooling and that the latter affects the conformation of the molecule. The loops may act as favourable entanglement sites for polymer coils flowing along the interface. New loops further extending into the solution in a second molecular layer may easily be formed by reptation of long chains through neighbouring loops of the adsorbed molecule. Since the first loop layer is firmly attached to the surface it is conceivable that in this manner an "entangled-layer" is generated with an exceptionally long life-time. Shear flow provides the necessary transport of the very long chains over these potential entanglement sites and thereby accelerating the gel formation. Two additional factors may be of importance in this gelation step. First of all the state of supercooling of the solution leads to the tendency of the chain segments to form embryonic crystallites, or heterophase fluctuation as described by Frenkel (44). These crystallites are likely to extend the life-time of these entangled aggregates. The second factor is the stretching effect of the hydrodynamic field which accelerate the tendency to crystallize due to chain alignment. Obviously it is difficult to assess to what extent these transient crystallites increase the disengagement time of the network. Furthermore we have not yet taken into consideration that in normal-stress fluids, as these supercooled entangled polymer solutions are, secondary flow phenomena (36,43,45) occur already at relatively low shear rates and may possibly induce some fibrous crystallization. Another observation that corroborates this picture of the mechanism of gel formation is the remarkable effective molecular fractionation that takes place in stirred solution crystallization (46,79,81) even in rather highly concentrated solutions. This finding points to the fact that the longest molecules are preferentially incorporated into the gel. This selection process of the

very large molecules can be accounted for by an increase in life-time of an entanglement with increasing strand length (100). This will especially be the case for the large molecules being entangled in several loops.

In this context reference should be made to studies of the negative thixotropy of aqueous solutions of polymethacrylic acid as reported by Eliassaf, Silberberg and Katchalsky (47). They found stirring induces gellation in these solutions and attributed this negative thixotropy to the formation of more intermolecular bonds in a flow-field. A more directly related observation is the anomalous streaming birefringence which occurs when polyethylene solutions are supercooled as reported by Janeschitz-Kriegl (48). Similar apparent anomalies were noticed by Munk and Peterlin (49) who studied the time dependence of streaming birefringence of polystyrene solutions in viscous solvents like aroclor and concluded that entangled aggregates of several molecules should be formed in flow fields.

Returning to our model for fibrous growth as shown in Fig. 5, it is supposed to depict that the effectiveness of the stretching of the entanglement network is actually due to two factors. First of all the gel is attached to the rotor surface by the adsorbed layer on one end and connected to the seed crystal on the other end through reptation of cilia into the network meshes. Secondly the seed crystal and rotor surface move in opposite directions. Evidently, this complex mode of oriented crystallization of entanglement networks will be dependent on many variables such as take-up speed, rotor-speed, temperature, solvent quality and viscosity, polymer concentration, rotor surface roughness, etc. Several of these variables turned out to be interdependent.

A strong indication of the major effect of crystallization in this fiber formation process is the linear decrease of the fiber mass growth rate with increasing temperature. The action of the stress field on the crystallites in the fiber may be quite significant as judged from the observation that in the case the fiber breaks the portion attached to the rotor surface snaps back like a rubber band indicating that at the crystallization temperature the crystallites can disappear nearly instantaneously. Apparently lateral crystal growth, that provides the thermal stability to the crystallites, proceeds at a considerably slower pace. Another pertinent experimental result is that the mass growth rate increases linearly with rotor speed (16,51). One may have expected a quadratic dependence (45,53) on the rotor speed, since the increase in the driving force for crystallization arising from the elastically stored free energy is proportional to the square of the shear rate.

We also noticed that the wind-up tension in the fiber increases with crystallization temperature. This could point to a diminishing contribution to the stress relaxation from oriented crystallization and the necessity to achieve more extensive coil deformation for growth. At relatively high crystallization temperatures the fibers become thinner while the take-up tension just increases and this frequently leads to fiber fracture. Further investigations into the cause of fiber fracture (52) disclosed that the friction between fiber and rotor surface apparently makes up a considerable part of the wind-up tension. Growth interruption could also happen as a result of the fiber being wrapped several times around the rotor. By making a wedge-shaped groove in the rotor surface the latter cause of fracture could be eliminated.

In many experiments, fibrous growth was started at lower temperatures e.g. at 110°C for p-xylene solutions. Under these circumstances the nucleation of the seed crystal appeared to be less difficult and time-consuming and by raising the temperature, growth could be continued even at 125°C which is above the equilibrium dissolution temperature for unconstrained ideal polyethylene crystals of 118.6°C. This rather small difference in crystallization temperature turned out to have a tremendous effect on the morphology and the mechanical properties. The fibers produced at lower crystallization temperatures consist of agglomerates of elementary fibrils with a shish-kebab morphology as is shown by the scanning electron micrograph of Fig. 6. Growing fibers at higher temperatures e.g. around 120°C for p-xylene solutions and higher wind-up stresses resulted in smooth fibers as illustrated by the STEM electron micrograph of Fig. 7.

Apparently the stretching of polyethylene entanglement networks at lower temperatures is accompanied by the generation of long cilia which precipitate later-on as chain-folded platelets on the fibrous backbones (54), whereas at higher temperatures primarily backbone material is formed. Fast crystallization in the flow direction at lower temperatures gives rise to trapping defects such as entanglements and generates disordered domains from which the cilia emerge (55). At higher temperatures particularly in the early stages of slow crystallization when embryonic crystallites are interspersed by elastic chain strands, creep is likely to occur and cilia may possibly be pulled into the stretched by filament by sliding motions through entanglement loops. Also the transport of stems through these small crystallites contributes considerably to the removal of topological constraints and the release of stress concentrations.

Cilia could also be eliminated by subjecting shish-kebab fibers to a second-stage hot-drawing process (55-57). This transformation of lamellar material into fibrillar material is accompanied by an increase in tensile strength as is illustrated in Fig. 8 where the tensile strength, for a shish-kebab polyethylene fiber prepared by the "surface growth" technique, is plotted versus the drawing temperature. Low drawing temperature upto 100°C appear to be less effective in accomplishing an increase in strength, but in the range from 120°C to 145°C where there is sufficient chain mobility in the orthorhombic crystallites, the strength enhances from 1.9 GPa to 3 GPa.

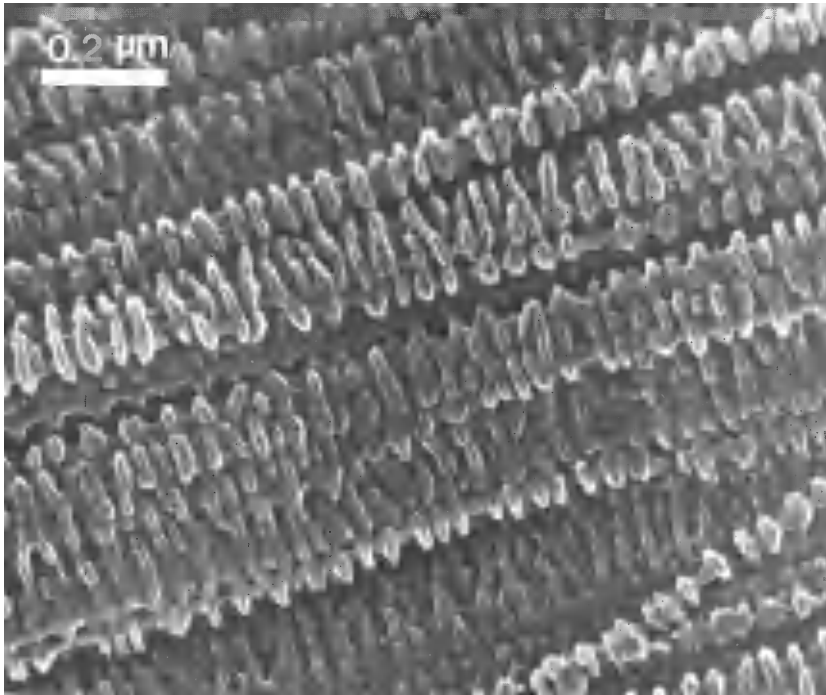


Fig. 6. SEM-micrograph of a "surface-growth" fiber produced at a crystallization temperature of 110°C in p-xylene, revealing a typical shish-kebab morphology.

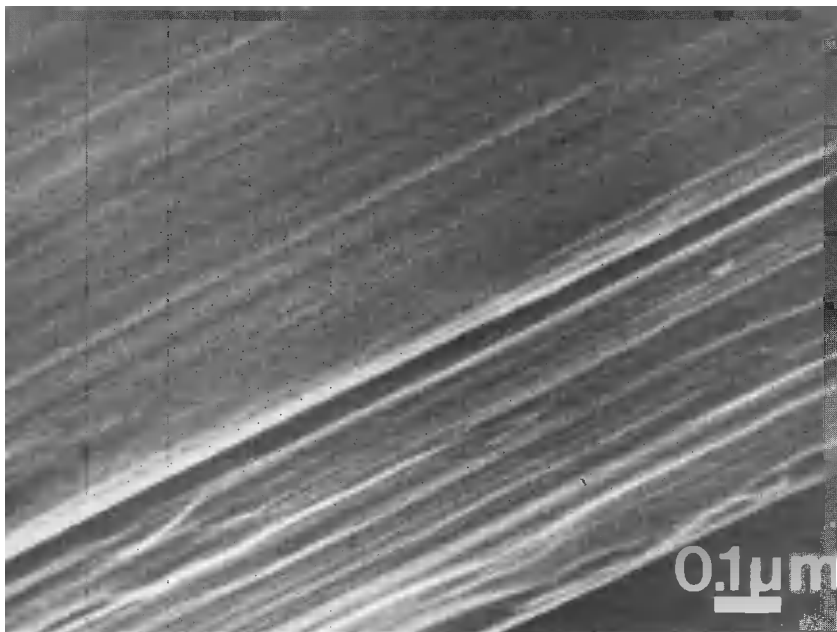


Fig. 7. SEM micrograph of a hot-drawn "surface-growth" fiber showing a fully oriented smooth fibrillar structure. Similar morphologies are generally observed in "surface-growth" fibers produced at high crystallization temperatures.



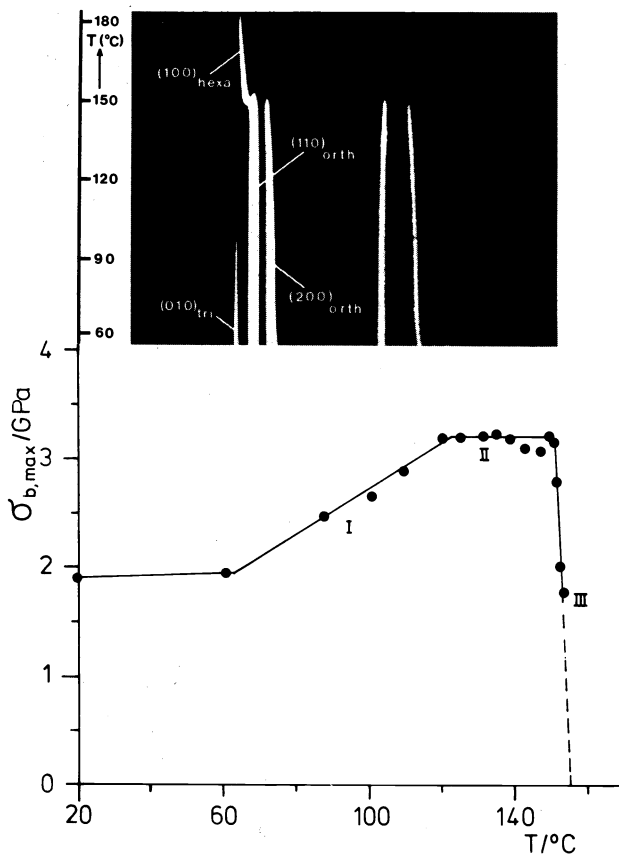


Fig. 8. The lower part shows the tensile strength at break  $\sigma_b$  after hot-drawing of "surface-growth" fibers as a function of drawing temperature. The upper part shows an equatorial wide-angle X-ray diffractogram of a constrained "surface-growth" fiber continuously recorded at increasing temperature. The heating rate was 0.35°C/min. Note the transition of the orthorhombic (110) and (200) reflections into the (100) reflection of the hexagonal phase at 150°C, which results in a drastic decrease of the tensile strength upon hot-drawing.

The ultimate tensile strength achievable was 5 GPa for shish-kebab fibers with an initial strength of 2.4 GPa. Therefore in addition to the temperature also the structure of the fiber prior to drawing and especially the topology of the entanglement network are important in attaining high strength values. Swelling (58) the shish-kebab fibers in p-xylene at 118°C to remove 15% of the low molecular weight tail of the distribution and having in the gel only the very largest molecules had unexpectedly a negative effect on the drawing. Strengths of only 2.8 GPa were obtained and this poor result, in comparison to the strength of 4 GPa initially obtained after hot-drawing, may be due to the removal of certain entanglements which are necessary for accomplishing ultimate alignment of the molecules. Hot-drawing of these shish-kebab fibers at temperatures beyond 150°C results in an abrupt decrease in strength. This seems to be associated with the transformation of the orthorhombic crystal lattice into the hexagonal structure at 150°C (15,57) in which the chains start to oscillate around their axis and easily slip past each other. Rather small drawing forces are then sufficient for the disengagement of entanglement by chain segment transport through rapid movements of Reneker point defects (27) along the molecules. Disruption of the entanglement network which provides the essential connectiveness between the molecules may be the cause of the rapid drop in strength.

One of the limitations of the "surface-growth" technique so far encountered is that the fiber growth rate appears to be rather small. The highest value for the polyethylene fiber production rate achieved with our equipment was 150 cm/min. Since this limiting value is due to fiber fracture, caused for a significant part by the friction between the fiber and the rotor surface, we decided to look for other techniques which avoid the friction, but utilizes the principle of stretching entanglement networks under controlled conditions of temperature, deformation rate, network topology and solvent quality.

For this reason Kalb (17) started to investigate the potential of the so-called gel-spinning or gel-extrusion spinning as a technique for producing strong fibers.

### Gel-spinning

Gel-spinning of high molecular weight polyethylene goes at any rate back to investigations by Zwick (59) who described this method and variants such as phase separation spinning in 1967. The term gel-spinning actually refers to the fact that polymer concentrations of 30 to 50 % are used (39) and that the solvent in this case better be regarded as a plasticizer. This gel extrusion techniques allows fiber production speeds of as high as 500 m/min. Obviously there are quite a number of routes for transforming these gels into a filament. For instance Frenkel and Baranov et al. (60,61) described how moderately concentrated polymer solutions can be converted into fibers simply by pulling a thread from the solution meniscus and wind it up on a drum. Several aspects of the self-hardening of polymer solutions in elongational flow-fields have been described by Ziabicki (39). In addition to the filament formation from the dissolved state of the polymer there are also processes in which the fiber is produced from partially crystalline gels.

For instance we spun fibers from xylene solutions of high molecular weight polyethylene (62, 63) and stretched the partially crystalline gels over a hot-plate thereby making a very strong fiber with a good knot-strength. Porous fibers of high molecular weight polyethylene were manufactured by spinning xylene solutions into flowing silicone oil at 95°C (63). Silicone oil is a nonsolvent for polyethylene and is miscible with xylene. This wet spinning process produced porous fibers which turned out to be highly deformable.

In this context it is pertinent to mention the dry-spinning process known as flash-spinning as developed by White and Blades (24,64) in 1963. They dissolved some 15 wt. % linear polyethylene in either methylenechloride or cyclohexane at temperatures in the range of 200 to 220°C and pressures of about 100 atmospheres. The viscosity of these superheated solutions is rather low and they can be spun with very high speeds (9000 m/min.) through orifices of 1 mm in diameter. The porosity and fibrillation due to expansion of the superheated solvent may be regulated by adding filler nucleating agents. Hot-drawing of these porous structures results in fibers and films known by the trade name Tyvek (108) and finds application in e.g. very light air-mail envelopes.

In our approach to adapting gel-spinning techniques (17-20,22,23) we have tried to find out which of all the variables involved is of prime importance for reaching high values of the tensile strength. Several solvents have been used such as dodecane, decaline, trichlorobenzene and p-xylene, but a large number of experiments have been carried out employing paraffin-oil. A schematic representation of successive operations involved in the gel-spinning/hot-drawing of very high molecular weight polyethylene is given in Fig. 9.

The first step in this process consists of dissolving 5 wt. % polyethylene powder in paraffin-oil at 150°C for 48 hours. Mild stirring is applied as long as the powder particles are visible. These rather long dissolution times seem to be favourable in order to obtain a homogeneous entanglement network. The gel, after being cooled down to room temperature, is fed into an extruder equipped with a long conical die of 10 cm in length, an entrance angle of 6° and an exit diameter of 1.8 mm or 0.8 mm (20,23). This extremely long die with very

DEL SPINNING / HOT DRAWING OF HIGH MOLECULAR WEIGHT POLYETHYLENE.

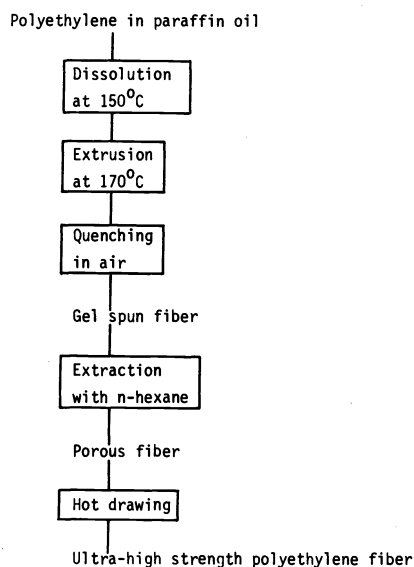


Fig. 9. Schematic representation of the gel-spinning/hot-drawing process.

small entrance angle has been selected in order to minimize the severity of extrudate distortion due to melt fracture (37,65).

The strongest fibers were spun at 170°C and rather small extrusion rates of about 1 m/min. These gel filaments were subsequently extracted with n-hexane, dried and hot-drawn at 148°C to draw ratio's of about 70. Tensile strengths at break of 4.1 GPa and Young's moduli of 160 GPa at room temperature could be obtained (20,23). Apart from the influence of polymer concentration, molecular weight distribution, solvent quality and temperature, extrusion rate, die-shape on the gel-spinning one should expect to find a strong dependence of the properties of the as-spun fiber on the flow rate (23). In particular in the case of high molecular weight polymers flow instabilities such as die-swell, elastic turbulence or melt-fracture and spiral flow are bound to be encountered even at very small extrusion rates. It seems to be well accepted that the onset of elastic turbulence is related to a critical shear stress at the wall of the die (65), which is inversely proportional to the molecular weight of the polymer (66,67). It is also clear that these elastic turbulence phenomena, which inevitably lower the strength of the fiber, only occur in the case of an effective entanglement network. Since the frequency and efficiency of the entanglement couplings increase with molecular weight it need not be surprising that the high molecular weight polyethylene solutions are particularly sensitive to the occurrence of melt-fracture (68,69, 100). These flow disturbances may be suppressed by using a conical die to reduce the elongational flow gradient at the die entrance (34) by employing additives (37,68) and by pulling the extrudate immediately after leaving the die.

The influence of the stretching rate and some additive on the tensile strength has been examined (23) and some of the results are shown in Fig. 10. The tensile strength at break,  $\sigma_b$ ,

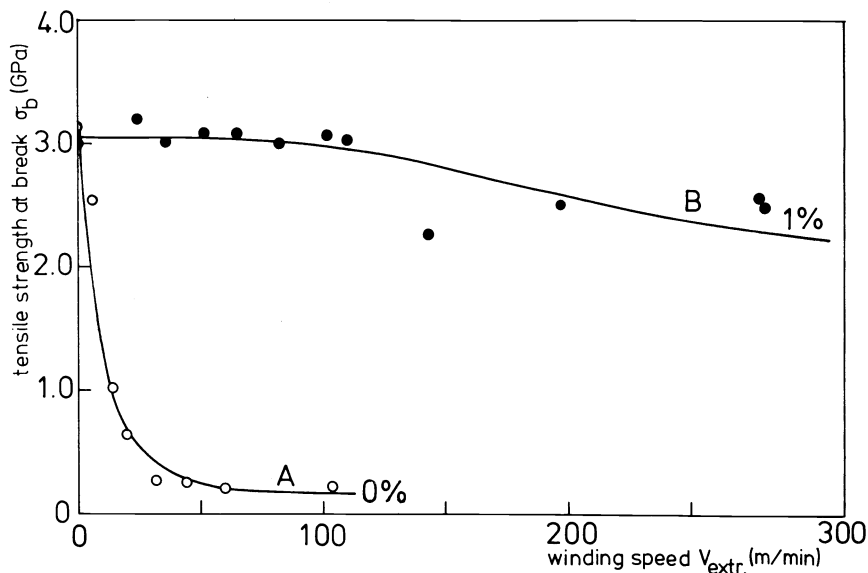


Fig. 10. Tensile strength at break after hot-drawing vs. take-up speed during gel-spinning at different concentration of Al-stearate (wt. %) in the spinning solution.

after hot-drawing of the filaments, as a function of the take-up speed during extrusion of a 5 wt. % solution of high molecular weight polyethylene in paraffin-oil exhibits a marked decrease in strength already at 10 m/min. (curve A in Fig. 10). It should be noted that the stretching action of the extrudate actually amounts to pulling the gel from the interior of the die. This could effectively lead to an increase in shear stress at the wall. Adding 1 wt. % of aluminium-stearate to the paraffin-oil had surprisingly an enormous effect on the strength-wind-up speed relationship. Even up to 270 m/min the tensile strength level was still of the order of 3 GPa (curve B in Fig. 10) and gel wind-up speeds of 800 m/min were feasible. We are inclined to attribute this large effect for a considerable part to the reduced adsorption of the very large polyethylene molecules on the wall of the die by adding the aluminium-stearate. Without the additive the adsorbed polyethylene molecules form loops which are favourable entanglement sites for the generation of new entangled layers by reptation. The longer life-times of these entanglements is readily apparent from the fact that a firmly attached gellayer is formed on the wall of the die after spinning. Using the additive leaves a clean die after spinning and also results in a deformation of the fluid filament outside the die, instead of inside. The aluminium-stearate increases the viscosity of the solvent and this affects the life-time of the entanglements and the coil extensibility.

In this more viscous fluid the tendency to generate elastic turbulences is likely to be suppressed but this additive may also reduce neck formation and involves a kind of superplasticity, which promotes the homogeneity of the filament at rather high elongations. High-speed extrusion-drawing also produces a high degree of orientation in the as-spun fiber. The morphology is that of shish-kebabs (23) which can be further extended upon hot-drawing. If the extrusion draw-ratio is multiplied by the additional hot-draw ratio an overall value of about 1500 is obtained. This implies that in the combined process the deformation cannot be affine. In other words the fiber formation cannot exclusively be due to extension of the coils participating in the entanglement network. Slippage of polymer chains past each other has to occur during these extrudate drawing experiments. Since shish-kebabs appear to be present in the as-spun gels it is conceivable that during the flow of the doped solutions, resembling superplasticity (70), flow units are formed containing the molecules in strongly entangled aggregates as present in the elementary fibrils with shish-kebab morphology. These flow units are surrounded by fluid layers that contain polymer molecules which form only short life-time entanglements with chains in neighbouring units. This may be closely analogous to flow units proposed by Mooney (71) and to cluster flow (72) described by Williamson and Busse (69,73) and the fluid filaments suggested by George (74). Irrespective of the view on the detailed mechanism one may infer that the entanglement network as present in the original gel prior to spinning need not necessarily be preserved in order to produce a high strength fiber.

#### Hot-drawing

Hot-drawing also has a strong effect on the fiber strength and one should therefore examine how the transformation of the porous fiber after spinning into a strong filament proceeds and depends on drawing variables such as temperature, drawing-rate and stress (22). Figure 11

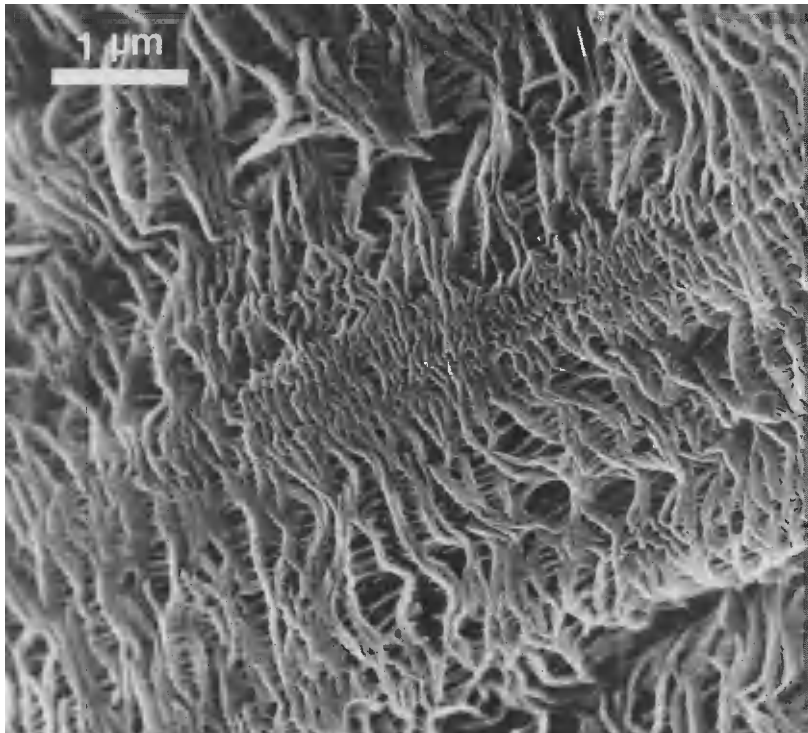


Fig. 11. SEM-micrograph of an extracted as-spun filament obtained from a 5 wt. % solution of ultra-high molecular weight polyethylene in paraffin-oil (extrusion rate 0.75 m/min).

shows a scanning electron micrograph of an extracted fiber produced from a 5 wt. % solution of the polyethylene in paraffin-oil at an extrusion rate of 0.75 m/min at 170°C (23). The morphology of this filament consists of loosely connected large lamellae. The connections between these lamellae consist of a number of more or less parallel fibrils apparently produced by some slight orientation, accomplished in the course of spinning. In visualizing how the hot-drawing process proceeds one has to bear in mind that the entanglement network of the original gel is superimposed on the lamellar aggregate of Fig. 11. This morphology is transformed into a bundle of parallel oriented shish-kebabs for gels, spun at high extrudate wind-up speeds (23). The change in morphology of the lamellar fiber by drawing through a pipe at 148°C under a gentle stream of pure nitrogen has been investigated by transmission electron

microscopy of fiber fragments and by Small-angle X-ray scattering (75). These hot-drawn fibers can be dispersed at various stages of drawing by nitric acid etching followed by ultrasonic agitation.

Figure 12 shows that the fiber fragments after drawing to a ratio of 5.6 clearly have a

PE gel-spun fibre hot drawn at 145°C to various draw ratios  $\lambda$

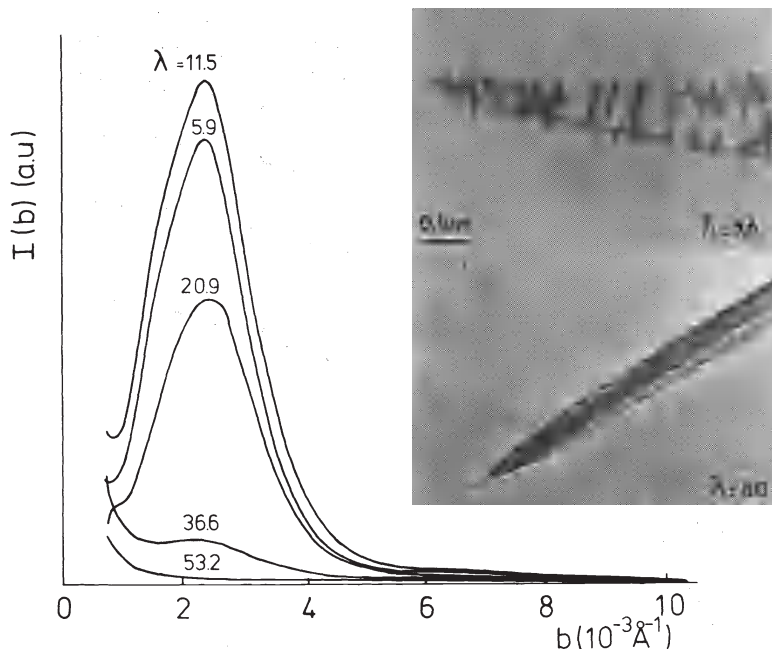


Fig. 12. Transmission electron micrographs of fragments obtained by nitric acid etching of gel-spun fibers drawn to different draw ratio's  $\lambda$  at a drawing temperature of 145°C. Also SAXS-curves of this fiber at different draw ratio's are presented.

shish-kebab morphology. Since the porosity of the starting filament is completely lost the large lamellae connected by a few fibrils must have been converted into a new morphology as an intermediate structure. Hot-drawing to a ratio of 80 yield nearly completely smooth elementary fibrils. Here again we run into the same phenomenon as observed in the case of the "surface-growth" process, namely the fully drawn structure consists of smooth fibers and intermediate structures display a shish-kebab morphology.

Small-angle X-ray scattering (SAXS) curves of these gel-spun fibers drawn to various values of  $\lambda$  essentially confirm this picture (75). For moderate draw-ratio's these SAXS-curves, presented also in Fig. 12, exhibit a clear Bragg-peak corresponding to a long period of 400 Å. This scattering is not due to the presence of voids since fibers immersed in liquids exhibited the same scattering pattern and intensity. The long period of 400 Å is very likely to be due to lamellar overgrowth of fibrillar crystals, since these scattering curves are identical to those of shish-kebabs produced by melting and recrystallizing of "surface-growth" fibers. The highly drawn fibers,  $\lambda > 60$ , do not exhibit a maximum in the SAXS-curve, indicating that the shish-kebabs as an ever emerging intermediate polymer morphology have completely been transformed into smooth fibrils.

The molecular mechanism associated with the alignment of the polyethylene molecules in the hot-drawing process, however, is still rather obscure. In order to gain a better understanding of the deformation process, we determined the activation energy acquired by the flow units in hot-drawing by measuring the elongational viscosity,  $\eta_e$ , as a function of temperature and draw ratio (22). Isothermal elongation experiments were performed at fixed tensile speeds in the range of  $10^{-6}$ - $10^{-3}$  m/s and in the temperature range 100-150°C, yielding actually an apparent elongational viscosity. The latter quantity was determined by

$$\eta_e = \sigma_{xx} / \dot{\epsilon} \quad [1]$$

where  $\sigma_{xx}$  is the axial tensile stress,  $\dot{\epsilon} = \lambda^{-1} \cdot d\lambda/dt$  is the deformation rate and  $\lambda$  is the draw ratio. From the elongational viscosity the apparent activation energy can be derived using the equation

$$\eta_{\epsilon}(T) = \eta_{\epsilon}(T_0) \cdot \exp \{E_a/R \cdot (T^{-1} - T_0^{-1})\} \quad [2]$$

where  $E_a = U - \sigma_{XX} \cdot V^*$  is the apparent activation energy and  $V^*$  is the activation volume. The apparent elongational viscosity is strongly dependent on the draw ratio and the deformation rate. Therefore values of  $\eta_{\epsilon}$  for fixed values of  $\lambda$  and  $\dot{\epsilon}$  at different temperatures are compared in Fig. 13 where  $\ln \eta_{\epsilon}$  is plotted versus  $T^{-1}$ . There are three distinct temperature

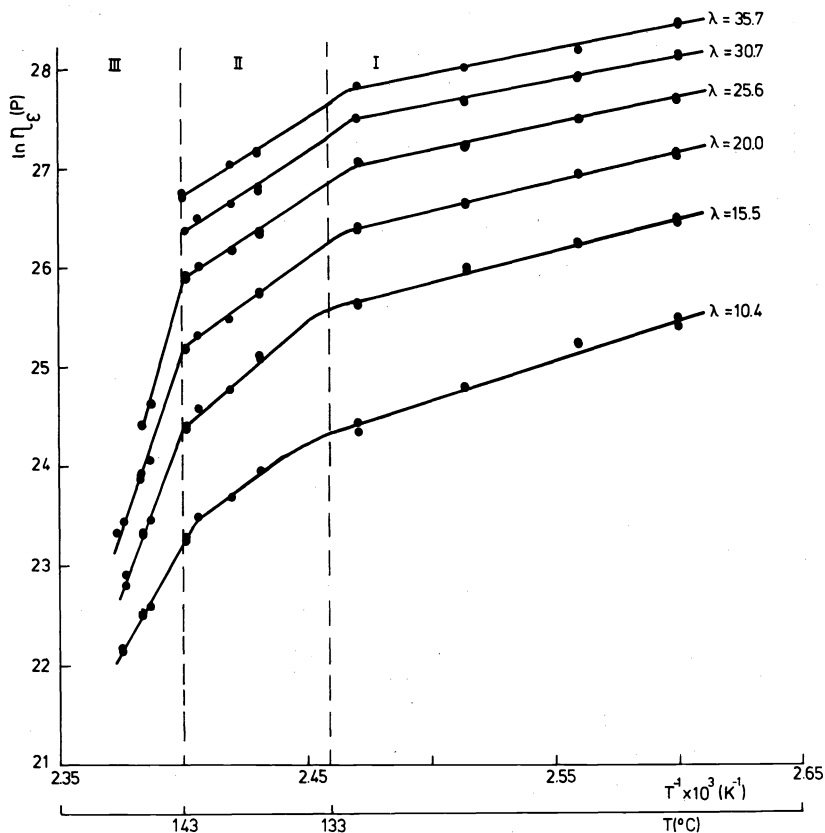


Fig. 13. Plot of logarithm of apparent elongational viscosity,  $\ln \eta_{\epsilon}$ , versus reciprocal temperature  $T^{-1}$  at several draw ratio's for the determination of activation energy  $E_a$ .

regions as judged from the different slopes of the linear relationship between  $\ln \eta_{\epsilon}$  and  $T^{-1}$ . It should be remarked that the fibers used for elongational viscosity measurements were previously drawn to  $\lambda = 10$  and the activation energies therefore refer to the transformation of shish-kebabs into smooth fibrils.

A low temperature region can be distinguished up to a temperature of 133°C in which the flow process requires an activation energy of 50 kJ/mole. This process is presumably associated with the flow of separate fibrils and the unfolding of blocks of chain-folded lamellar crystals. In the temperature range between 133°C and 143°C the activation energy was found to be 150 kJ/mole and is again independent of draw ratio. In this temperature region the lamellae melt and the fibrils aggregate. The melt of cilia surrounding the backbones will inevitably increase the energy barrier for the drawing process. In the third temperature regime between 143 and 148°C, the activation energy is in the range of 300-600 kJ/mole, dependent on draw ratio. The mobility of the chains is sufficient to allow slippage of individual stems through the crystal lattice and the release of stress concentrations by the rapid transport of Reneker point defects (27) along the chains. In this regime the entanglements may act as semi-permanent crosslinks providing the necessary coherence between the molecules (23,80). The transport of also topological defects along the fiber axis gives rise to an increase in crystallite dimensions in the chain direction up to about 800 Å (76). These three temperature regimes and molecular rearrangements have been schematically presented in Fig. 14. Apart from the temperature also the deformation rate has a strong influence on the elongational viscosity behaviour of these semi-crystalline polyethylene filaments. Figure 15 presents the linear dependence of  $\ln \eta_{\epsilon}$  on  $\ln \dot{\epsilon}$  and illustrates the decrease of the elongational viscosity with strain rate. This is similar to the flow of other systems and poly-

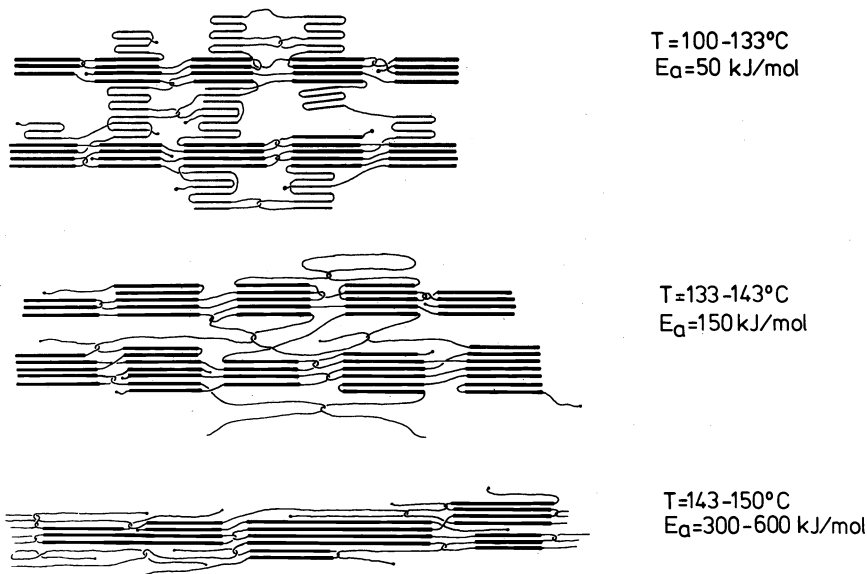


Fig. 14. Schematic representation of the deformation mechanism during hot-drawing in three different temperature regions with a different apparent activation energy.

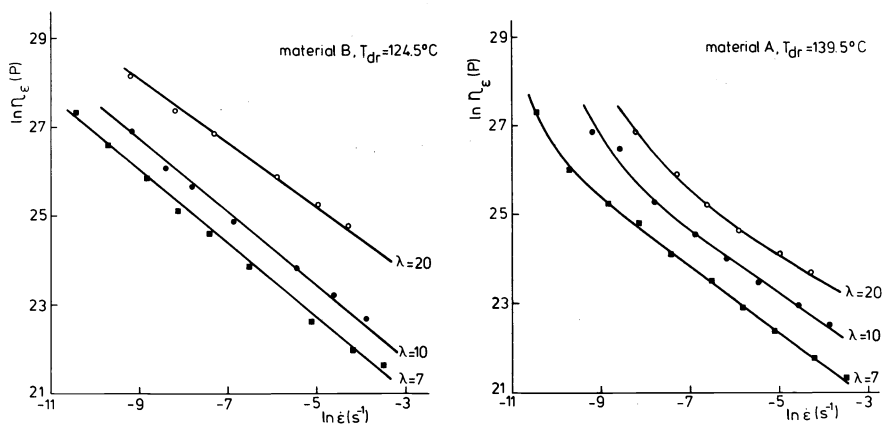


Fig. 15. Dependence of the apparent elongational viscosity  $\eta_e$  on deformation rate  $\dot{\epsilon}$  for two different sets of gel-spun fiber at different draw ratio's and temperatures (Fig. 15A:  $T = 124.5^\circ\text{C}$ ; Fig. 15B:  $T = 139.5^\circ\text{C}$ ).

ethylene melts and is referred to as strain softening behaviour (77). In analogy with the model of Marrucci and Hermans (78) which is basically derived for polymer melts one may consider the decrease of  $\eta_e$  with  $\dot{\epsilon}$  for several values of  $\lambda$  as a result of the flow units becoming more elongated.

#### EVIDENCE FOR THE DOMINANT ROLE OF ENTANGLEMENTS.

In the preceding sections it has become evident that the influence of molecular entanglement couplings on the spinning and drawing behaviour of high molecular weight polyethylene can hardly be underestimated. This section emphasizes further evidence for the prevailing action of entanglements, although their presence cannot directly be demonstrated. In a homogeneous polymer solution such as the 5 wt. % solution of high molecular weight polyethylene in a good solvent as paraffin-oil, the molecular weight between entanglements,  $M_e(\text{sol})$ , is related to the volume fraction of the polymer,  $\phi_p$ , through (82)

$$\bar{M}_e(\text{sol}) = \bar{M}_e(\text{melt}) \cdot \phi_p^{-3/2} \quad [3]$$

where  $\bar{M}_e(\text{melt})$  stands for the molecular weight between entanglements in the undiluted polymer. Since  $\bar{M}_e(\text{melt})$  equals  $2 \cdot 10^3$  kg/kmol (89) one finds for a 5 wt. % solution of polyethylene in paraffin-oil, with  $\phi_p \approx 0.06$ , a value for  $\bar{M}_e(\text{sol})$  of  $17 \cdot 10^3$  kg/kmol. This implies that on the average, since Hifax 1900 has a number average molecular weight of about  $200 \cdot 10^3$  kg/kmol, there are approximately 12 entanglements per chain.

If one wants to know what happens to the network topology during spinning and subsequent hot-drawing the number of entanglements in the drawn fiber should be known. We assessed the entanglement concentration in the ultra-high strength polyethylene fiber by means of the following method (83,84). A fiber with an initial strength of 3 GPa was crosslinked by applying varying doses of  $^{60}\text{Co}$   $\gamma$ -irradiation from 6 to 70 kGy (1 kGy = 0.1 Mrad). The gel content,  $w_g$ , increased from 0.54 to 0.81. The number of effective network chains in the gel,  $\nu_g^*$ , was calculated using the recent swelling theory developed by Flory (85,86) and the degree of swelling determined in p-xylene at 120°C. In order to determine the number of elastic chains per unit volume of the original fiber before extraction,  $\nu^*$ , one has to use the equation (87,88)

$$\nu^* = \nu_g^* \cdot w_g \quad [4]$$

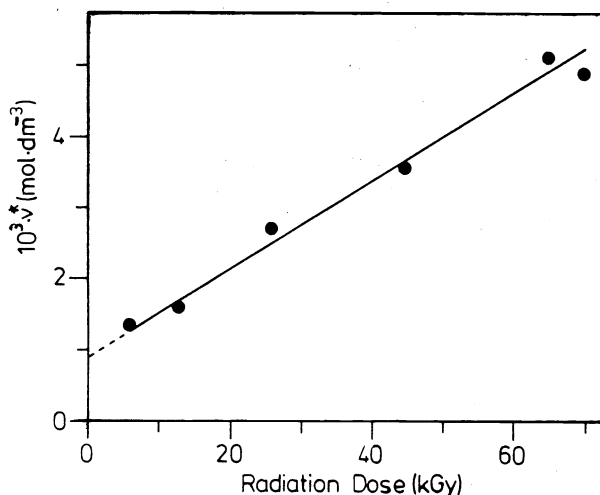


Fig. 16. Effective network chain density,  $\nu^*$ , as a function of  $\gamma$ -radiation, for a polyethylene fiber with an initial tensile strength at break of 3.0 GPa.

The values for  $\nu^*$  have been plotted versus radiation dose in Fig. 16 which illustrates that there is a positive intercept after extrapolation to zero dose, implying that entanglements must be present in the fiber (87). As a result of chain fracturing during irradiation and the broad molecular weight distribution, not all entanglements will be trapped in the crosslinking process. Using Langley's theory (87) for the number of elastic chains in irradiated polymers, we calculated for the higher radiation doses an entanglement concentration of  $1 \cdot 10^{-2}$  mol/dm<sup>3</sup>. This amounts to a molecular weight between entanglements of  $100 \cdot 10^3$  kg/kmol. For a number average molecular weight of  $200 \cdot 10^3$  kg/kmol in the original fiber this yields 2 entanglements per chain. Comparing with the 5% gel having 12 entanglements per chain, spinning combined with hot-drawing indeed markedly reduces the entanglement density (80). It need not be necessary to emphasize that the entanglement densities mentioned here are rough estimates and for instance the influence of the solvent quality on the number of entanglements (90) that induce elastically active chains, as well as the effect of the ori-



ginal molecular weight distribution (91) and the crosslinking mechanism for the irradiation of these fibers should be taken into account.

Another way to demonstrate that entanglements are preserved in the course of the fiber formation is to investigate the superheating effects of fibers loaded in tension, while they are exposed to solvents like p-xylene (92). Freely suspended polyethylene fibers were found to dissolve at 119.5°C. But when a stress of 30 MPa was applied the fiber could withstand a temperature of 132°C for at least two days. At still higher temperature the applied stress relaxed almost completely and dissolution occurred immediately after the fiber broke. The stress relaxation as a function of time for various temperatures of which the polyethylene fibers were exposed to p-xylene shown in Fig. 17, clearly demonstrate the marked superheata-

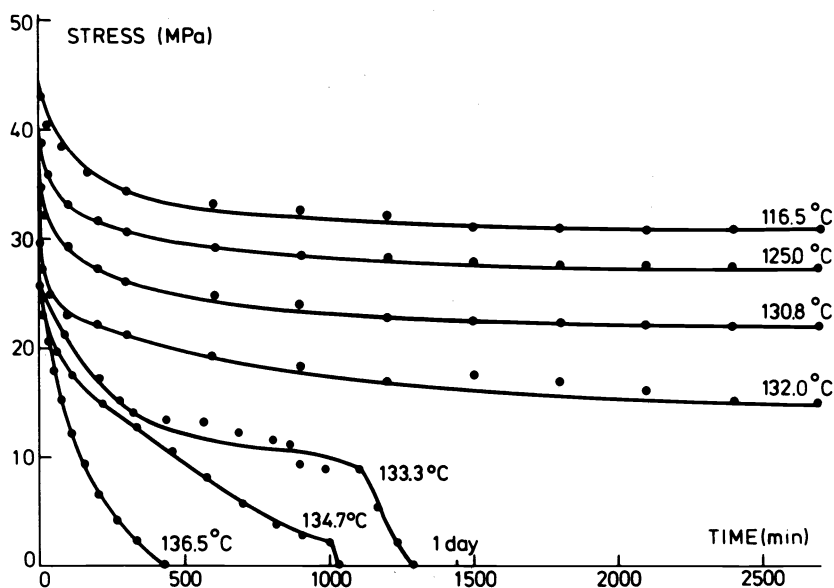


Fig. 17. Stress as a function of time for a polyethylene fiber, with an initial tensile strength at break of 3.0 GPa, immersed in p-xylene at various temperatures.

bility. At first glance this phenomenon should be attributed to the suppressing of the swelling of the disordered domains in p-xylene by the applied stress. However in these polyethylene fibers the continuous backbone structure is also loaded in tension. The thus increased free energy should increase the tendency of the fibers to dissolve. If this does not happen even at temperatures as high as 132°C it necessarily leads to the conclusion that the molecules are connected by trapped entanglements and twist disclinations.

Other crystalline fibers of polymers such as poly(L-lactide), display the effect of entanglements in the course of fiber formation in a rather pronounced manner (93). For instance, when a 20 wt. % solution of poly(L-lactide), abbreviated as PLLA, in chloroform is spun at 25°C at an extrudate rate of about 1 m/min, a very regular helical structure is produced as demonstrated by the scanning electron micrograph of Fig. 18. Spiral-flow is only observed in the case of rather strongly entangled polymer systems (34,69). Upon hot-drawing at 200°C these helical surface structures are gradually extended as a function of the draw-ratio and at  $\lambda = 20$ , the spiral is completely extended as shown by the schematic representation in the upper part of Fig. 19. But when the extended helix is again exposed to the drawing temperature of 200°C without any stress, the fiber immediately shrinks back to the initial non-deformed helical state with the same pitch, as illustrated by the SEM micrograph in the lower part of Fig. 19. This strongly indicates that the entanglement network, which is responsible for the occurrence of the helical fiber, is also to a large extent preserved in this hot-drawing experiment.

Finally the influence of the PLLA-concentration on the tensile strength at break (93) will be discussed. In Fig. 20 a plot is given of the tensile strength for PLLA-fibers versus the reciprocal of the polymer volume fraction,  $1/\phi_p$ . This quantity varies from 1 for purely melt-spun fibers to 0.01 for the 1% solutions. The molecular weights were in the range between  $180 \cdot 10^3$  and  $600 \cdot 10^3$ . The melt-spun fibers all have a tensile strength of 0.5 GPa regardless of molecular weight. A marked difference shows up for the 5 wt. % solutions where a strength is attained of 1.2 GPa for the  $600 \cdot 10^3$  molecular weight. This solution apparently had the optimum number of entanglements.

In the 1 wt. % solutions the molecular weight between entanglements is approximately 100 times larger than in the melt. The strength of these fibers was very low of the order of

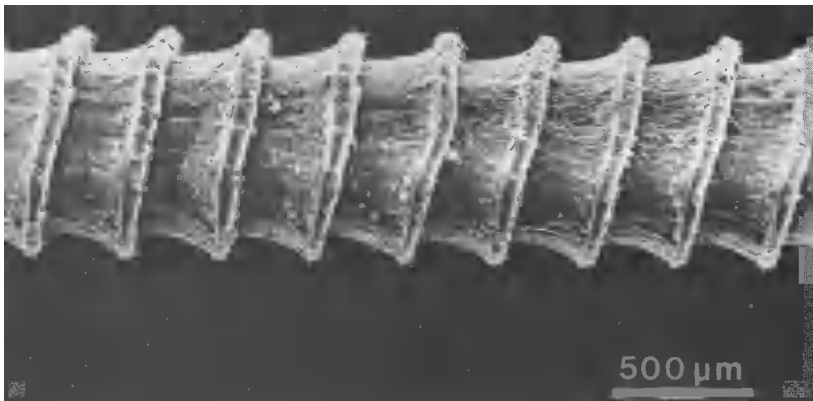


Fig. 18. SEM-micrograph of the surface of an as-spun PLLA-fiber. The fiber was spun from a 20 wt. % solution of PLLA (viscosity average molecular weight determined in chloroform at 25°C was  $600 \cdot 10^3$  kg/kmol). Spinning temperature was 20°C.

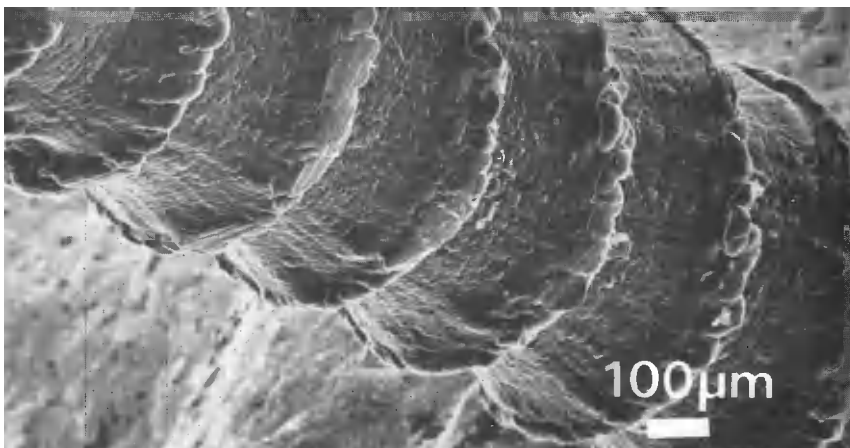
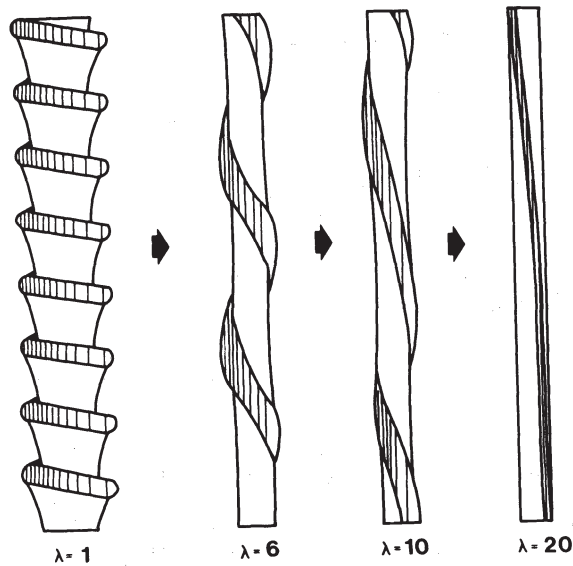


Fig. 19. Upper part: Schematic representation of the extension of a PLLA helical fiber upon hot-drawing. Lower part: SEM-micrograph of a shrunken hot-drawn PLLA-helix.

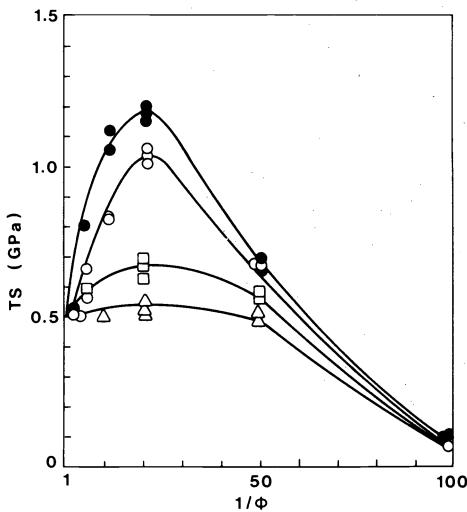


Fig. 20

Fig. 20. Dependence of the tensile strength at break, TS, of PLLA-fibers on the concentration,  $\phi$ , of the polymer solution used for spinning.  
 ●  $\bar{M}_V = 600 \cdot 10^3$  kg/kmol; ○  $\bar{M}_V = 500 \cdot 10^3$  kg/kmol; □  $\bar{M}_V = 350 \cdot 10^3$  kg/kmol;  
 △  $\bar{M}_V = 180 \cdot 10^3$  kg/kmol.

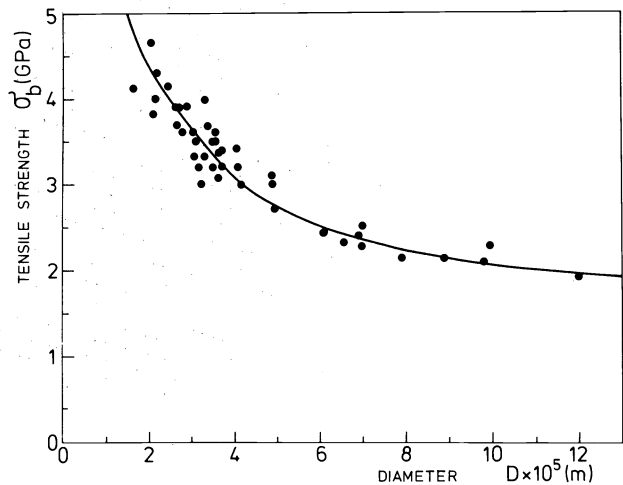


Fig. 21

Fig. 21. Tensile strength at break  $\sigma_b$  of fully oriented polyethylene filaments as a function of fiber diameter.

0.1 GPa. This clearly shows that if a sufficient number of entanglements in these gels are absent, stretching of the polymer coils in the hot-drawing experiment is virtually impossible. Therefore one cannot produce strong fibers. This observation is substantiated by the extraction experiments of high molecular weight polyethylene- and PLLA-fibers, where the low molecular weight species are allowed to diffuse out of the swollen fibers, as was described in a previous section. The remaining high molecular weight component was not able to yield a strong fiber, due to the destruction of the entanglement network.

## MECHANICAL PROPERTIES

So far we explored in previous sections the variables and experimental conditions, in the process of preparation of polyethylene fibers, that could improve the tensile strength. This section is concerned with the question of whether the apparently limiting experimental value of 5 GPa for the tensile strength at break, is to be regarded as the strength of ideal polyethylene crystals composed of infinitely long extended chains.

On the basis of a creep failure theory, Schaeffgen (8) estimated that the ultimate strength of linear polyethylene should be 3.7 GPa, close to our experimental limit. However, the experimentally observed strain at break of the strongest fibers is approximately 5%, whereas theoretical estimates, based on bond stretching and valence angle distortion calculations (94), amount to 33%. This large difference between experimental and theoretical value points to the presence of defects in the structure (28), which cause early failure when the fibers are tensile loaded. In general, fiber fracture may be due to the presence of impurities, internal structural defects, surface flaws, disordered domains and misalignment of crystallites (24). Also the strongest fibers contain disordered domains as judged from the crystallinity derived from D.S.C. measurements (95). The crystalline blocks may be of the order of 800 Å (76) and the crystalline orientation factor  $f_c$  is as high as 0.999, but the boundaries of the elementary fibrils always appear to display some irregularities. Also the appearance of fiber cross-sections, stained by the Kanig technique (96) using chlorosulfonic acid, suggest that the accessibility of these fibrils decreases towards the center (22). In Peterlin's model of highly oriented polymer fibers the ends of the micro fibrils are supposed to be primarily located on the outer boundary of the fibrils (97,98). They are most likely the source of defects where microcracks may nucleate in tensile loading experiments. When the fibers are etched by ion-bombardment or with chlorosulfonic acid, cracks perpendicular to the fiber direction or even complete circular cracks around the fiber may be observed, similar to the "onion-skin" effect in polyethylene fibers shown by Nadkarni and Schultz (99).

If indeed the surface flaws induce early fracture as in the case of glass fibers and fibrous single crystals of polydiacetylenes, examined by Young *et al.* (9), one may expect that also in the case of the strong polyethylene fibers the tensile strength depends on the fiber diameter. Figure 21 shows that the tensile strength of polyethylene fibers, with draw ratio's exceeding 50, indeed decreases with increasing diameter. The data in Fig. 21 were obtained

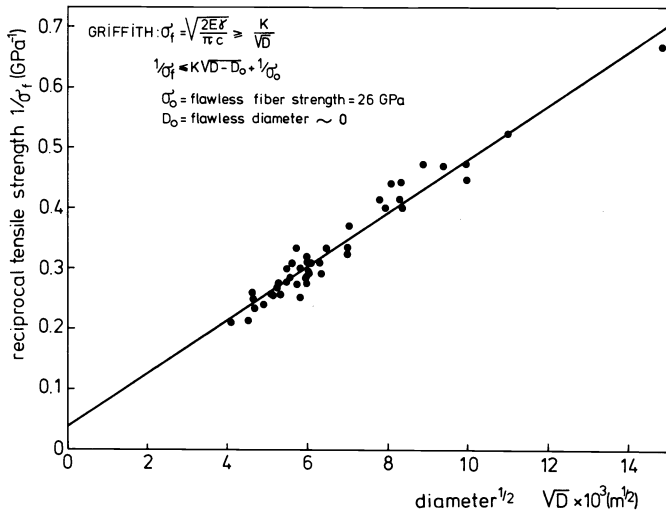


Fig. 22. Linear strength-diameter relationship as observed for ultra-oriented high molecular weight polyethylene fibers.

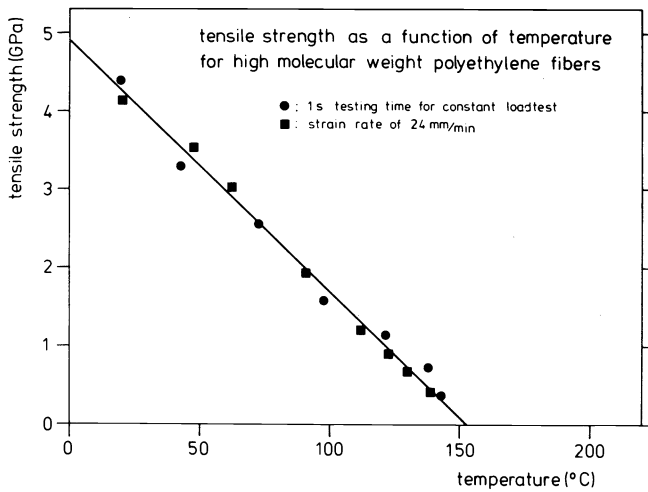


Fig. 23. Tensile strength at break,  $\sigma_b$ , as a function of temperature for an ultra-oriented polyethylene fiber.

on fibers produced by the "surface growth" technique, hot-drawing shish-kebab fibers, gel-spun fibers, including fibers spun from 20 wt. % solutions in paraffin-oil, which were drawn to  $\lambda = 100$ . Irrespective of the nature of the surface flaw and the relation of the stress concentration factor with the fiber diameter, the ultimate tensile strength,  $\sigma_0$ , of a polyethylene fiber without surface flaws can be obtained, according to Griffith (101), by plotting the reciprocal strength versus diameter. The corresponding equation reads

$$\sigma_b^{-1} = K (D - D_0)^{\frac{1}{2}} + \sigma_0^{-1} \tag{5}$$

where  $\sigma_b$  is the measured tensile strength at break and  $D_0$  is the diameter of a flawless fiber. The constant  $K$  is given by the Griffith law (101), if indeed fracture is due to a diameter dependent microcrack,

$$K = (2E\gamma/\pi)^{\frac{1}{2}} \tag{6}$$

where  $E$  is the Young's modulus and  $\gamma$  is the surface energy. A plot according to equation [5] yields a straight line as shown in Fig. 22 and extrapolates to a flawless fiber strength of 26 GPa for polyethylene. This sort of a value is to be expected since the theoretical value for the Young's modulus is somewhere in between 250 and 350 GPa and the strength should be about 1/10 (102) of this value according to a general rule-of-thumb. Boudreaux (94) calculated 19 GPa and Perepelkin (103) estimated 20-23 GPa using the Zhurkov (104) equation. So far annealing of these polyethylene fibers has never resulted in any significant increase in strength and it seems therefore reasonable to assume that the flaws are caused by topological defects (28).

Another observation that points to flaws of topological nature is that the helical fibers like the PLLA spiral have a lower strength than smooth fibers. The topological surface flaw may possibly originate from the elastic turbulence (34,69) generated by the highly elastic molecules and the adsorbed ones at the wall of the die. Limitations to the strength also arise from chain scission that was found to occur during gel-spinning/hot-drawing and in the

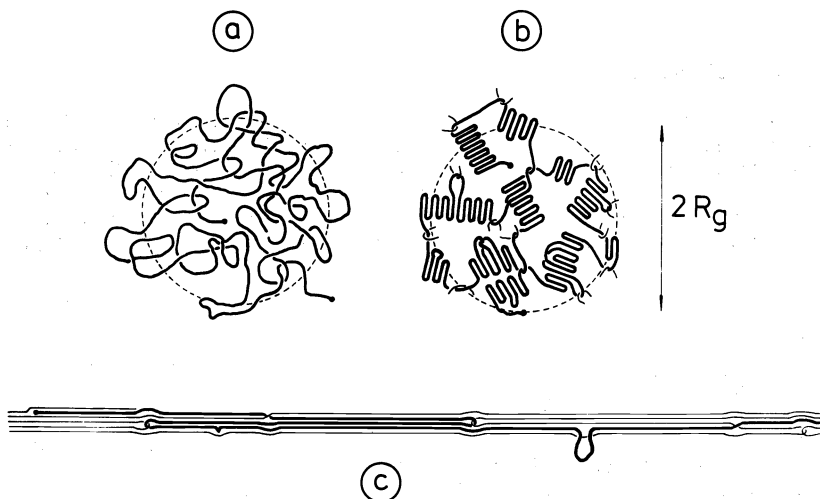


Fig. 24. Illustration of occurrences on the molecular level during solution preparation and drawing. a. A molecule in a semi-dilute polymer solution. b. Crystallization from solution, which may start at entanglement sites and trapping of entanglements. The radius of gyration  $R_g$ , remains approximately constant when crystallization takes place. c. Part of molecule which has generated numerous crystal defects in a drawn fiber.

course of fiber production (58) by the "surface-growth" technique. Finally the influence of temperature on the tensile strength should be briefly discussed. The data collected by Torfs (105) presented in fig. 23, exhibit a marked decrease in strength with temperature and the strength is zero at  $150^\circ\text{C}$ . Obviously the covalent bond between the carbon atoms is still strong at this temperature but these results indicate that fracture, may be more dependent on the pulling of chains out of the crystal lattice, as is underlined in Prevorsek's model (106), although some bond rupture is likely to be involved. It will be clear that these results are entirely in line with the predictions by Peterlin (97,98) that the lifetime of strained polymer fibers is not determined by the rupture of covalent bonds. According to this model, rupture will involve the translation of microfibrils past each other. Future studies may entail the development of strong fibers with increased temperature resistance. This may be accomplished either by starting from a polymer with a higher melting point such as poly(vinylalcohol), or by crosslinking polyethylene fibers by means of peroxides. Furthermore, since crosslinking introduces branched chains in the filaments, chain slippage may be minimized (107), thus increasing fiber life-time under constant loading. This interesting aspect will be dealt with in a future publication.

#### CONCLUSIONS

1. Ultra-high strength polyethylene fibers can be produced with a tensile strength level of 5 GPa and Young's moduli up to 200 GPa by starting from moderately dilute solutions of very large molecules by applying either the "surface-growth" technique or gel-spinning in combination with hot-drawing.
2. The "surface-growth" technique essentially consists of stretching a supercooled entanglement network by sliding a fibrillar seed-crystal through a gel, which is adsorbed on to the surface of the rotating inner cylinder of a Couette instrument. The limiting growth rate of the fibrous crystals is mainly determined by the take-up tension in the fiber due to friction with the rotor surface.
3. Gel-spinning encounters at higher extrusion rates the hydrodynamic instabilities such as die swell, elastic turbulence or melt fracture; these can largely be suppressed by employing additives such as 1 wt. % aluminium-stearate to a 5 wt. % solution of polyethylene in paraffin-oil. In that case spinning rates of 270 m/min are possible while still maintaining a strength level of 3 GPa after hot-drawing.
4. Hot-drawing of porous gel-spun fibers at  $145^\circ\text{C}$  to a draw ratio of 5.6 yields an intermediate morphology of the shish-kebab type, as disclosed by transmission electron microscopy of fiber fragments and by small-angle X-ray scattering experiments.
5. Further drawing results in a transformation of the shish-kebabs into smooth fibrils, which is thought to be feasible at high drawing temperature, as a result of sliding motions of cilia through entanglement loops and crystallites.
6. In the final ultimately drawn fiber there are still some entanglements left as revealed by swelling measurements of the fibers, crosslinked by  $\gamma$ -irradiation, and by the superheatability of the strained fibers in solvents.
7. The transformation of the entangled polyethylene molecules in solution into a fibrous crystal structure, in which the molecules are still connected by entanglements, are visualized in the models of Fig. 24.

## ACKNOWLEDGEMENTS

The authors are greatly indebted to Dr. J. Torfs, Drs. E. van der Wilt, W. Hamersma, H. Save-nije, J. Meijer and B. Klazema for their contributions to this work. Furthermore the authors would like to thank Dr. R. Huisman and Drs. M. Heuvel of ENKA-RESEARCH CENTER (AKZO) for many fruitful discussions and the determination of the fiber-crystallite dimensions as well as the crystalline orientation factor. Finally, Dr. P. van Duynen, is acknowledged for his ab-initio calculations on theoretical tensile strength at break of polyethylene fibers.

## REFERENCES

1. G.Capaccio, A.G.Gibson,I.M.Ward,"Ultra-High Modulus Polymers", A.Cifferri and I.M.Ward, Eds.,Applied Science Publishers, London,1(1979)
2. A.E.Zachariades, W.T.Mead, R.S.Porter, Chem. Rev., 80, 351(1980)
3. A.E.Zachariades, W.T.Mead, R.S.Porter, "Ultra-High Modulus Polymers", A.Cifferri and I.M.Ward,Eds., Applied Science Publishers, London, 77(1979)
4. G.Capaccio, T.A.Crompton, I.M.Ward, Polymer, 17, 644(1976)
5. E.S.Clark, L.S.Scott, Polym.Eng.and Sci., 14, 682(1974)
6. G.Capaccio, I.M.Ward, Polymer,18, 967(1977)
7. J.Preston, "Ultra-High Modulus Polymers", A.Cifferri and I.M.Ward,Eds., Applied Science Publishers,London,155(1979)
8. J.R.Schaeffgen, T.I.Bair, J.W.Ballou, S.L.Kwolek, P.W.Morgan, M.Panar, J.Zimmerman, "Ultra-High Modulus Polymers",A.Cifferri and I.M.Ward, Eds., Applied Science Publishers, London, 173(1979)
9. W.C.Wooten,Jr., F.E.McFarlane, T.F.Gray,Jr.,W.J.Jackson,Jr., "Ultra-High Modulus Polymers", A.Cifferri and I.M.Ward, Eds., Applied Science Publishers,London, 227(1979)
10. R.J.Young and C.Galiotis, Proc. IUPAC 1982 Amherst,640(1982)
11. D.N.Batchelder, C.Galiotis, R.T.Read and R.J.Young, Proc. of Conference on Deformation Yield and Fracture of Polymers, Cambridge, 21 (1982)
12. M.Iguchi, Brit. Polym. J., 5, 195(1973)
13. T.Kunugi, A.Suzuki, I.Akiyama and M.Hashimoto, Polym. Prepr., Am. Chem. Soc. Div. Polym. Chem., 20, 778(1979)
14. A.Zwijenburg, A.J.Pennings, Coll. and Pol. Sci., 254, 868(1976)
15. A.Zwijenburg, Ph.D-thesis, State University of Groningen, Groningen, The Netherlands (1978)
16. J.C.M.Torfs, A.J.Pennings, J. Appl. Polym.Sci. 26, 303(1980)
17. B.Kalb, A.J.Pennings, Polym. Bull. 1, 871(1979)
18. B.Kalb, A.J.Pennings, Polymer, 21, 3(1980)
19. B.Kalb, A.J.Pennings, J. Mater. Sci., 15, 2584(1980)
20. J.Smook, M.Flinterman, A.J.Pennings, Polym. Bull., 2, 775(1980)
21. D.W.Rabenhorst, T.R.Small and W.O.Wilkinson, John Hopkins University, Report no. DOE/EC/ 1-5085 (1979)
22. J.Smook, A.J.Pennings, J. Appl.Polym. Sci., 27, 2209(1982)
23. J.Smook, E.van der Wilt, A.J.Pennings, submitted to J. Appl. Polym.Sci.(1982)
24. E.E.Magat, Phil. Trans. R. Soc. Lond., A294, 463(1980)
25. P.J.Flory, J. Am. Chem. Soc., 67, 2048 (1945)
26. W.Pechhold, J. Polym. Sci., Part. C., 32, 123(1971)
27. D.H.Reneker, J. Polym. Sci., 59, 539(1962)
28. A.J.Pennings, J. Cryst. Growth. 48, 574(1980)
29. F.C.Frank, Phil. Mag., 42, 809(1951)
30. W.F.Harris, Sci. Am., 237, 130(1977)
31. R.L.Mc. Cullough, J. Polym. Sci., Phys. Ed., 15, 1805(1977)
32. P.Predecki, W.O.Statton, J. Appl. Phys., 38, 4140(1967)
33. M.Matsui, R.Masui, Y.Wada, Polym. J., 2, 134(1971)
34. J.P.Tordella,"Rheology",Vol.5, F.R. Eirich, Ed.. Academic Press. New York, 57(1969)
35. E.B.Bagley, H.P.Schreiber, ibid , 93(1969)
36. H.Gieskus, Rheol. Acta., 4, 85(1965)
37. C.D.Han "Rheology in Polymer Processing", Acedemic Press, New York (1976)
38. J.A.Brydson, "Flow Properties of Polymer Melts", George Goodwin Ltd., London(1981)
39. A.Ziabicki, "Fundamentals of Fibre Formation", Wiley, London, New York, Sydney(1976)
40. G.Marrucci, Polym. Eng. and Sci., 15, 229(1975)
41. A.J.Pennings, J.C.M.Torfs, Coll. and Polym. Sci., 257, 547(1979)
42. P.J.Barham, M.J.Hill, A.Keller, Coll. and Polym. Sci., 258, 899(1980)
43. A.J.Pennings, J.M.A.A. van der Mark, H.C. Booy, Kolloid Z.u.Z. Polymere, 236, 99(1970)
44. J.Frenkel,"Kinetic Theory of Liquids", Dover Ed., 382(1955)
45. A.J.Pennings, J. Polym. Sci., Polym. Symp., 59, 55(1977)
46. A.J.Pennings, "Characterization of Macromolecular Structure"(Proc. of the Washington Conf. (1967)), Natl. Acad. Sci., Washington, D.C., publ. No.1573(1968)

47. J.Eliassaf, A.Silberberg, A.Katchalsky, Nature, 193, 1119(1955)
48. H.Janeschitz-Kriegl., Adv. Polym. Sci., 6, 170 (1969)
49. P.Munk, A.Peterlin, Trans. Soc. Rheol., 14, 65(1970)
50. M.R.Mackley, G.S.Sapsford, "Developments in oriented polymers", I.M. Ward. Ed., Appl. Sci. Publ., in press
51. J.C.M.Torfs, A.J.Pennings, J. Appl. Polym. Sci., in press
52. J.C.M.Torfs, J.Smook, A.J.Pennings, J. Appl. Polym. Sci., 27, 5156(1982)
53. D.Acierno, F.P.La Mantia, G.Marrucci, Polym. Eng. Sci., 18, 817(1978)
54. P.F. van Hutten, A.J.Pennings, J. Polym. Sci., Polym. Phys. Ed., 18, 927(1980)
55. P.F. van Hutten, A.J.Pennings, Makromol. Chem. Rap. Comm., 1, 477(1980)
56. J.Smook, J.C.M.Torfs, P.F. van Hutten A.J.Pennings, Polym. Bull, 2, 293(1980)
57. J.Smook, J.C.M.Torfs, A.J.Pennings, Makromol. Chem., 182, 3351(1981)
58. J.Smook, A.J.Pennings, to be published.
59. M.M. Zwick, Appl. Polym. Symp., 6, 109(1967)
60. S.Ya. Frenkel, V.G. Baranov, N.G. Bel Nikevick, Yu.N.Panov, Vysokomol Soyed, 6, 1917(1964)
61. S.Ya. Frenkel, S.A.Agranova, V.G.Baranov, Yu.N.Panov, T.I.Samsonova, V.G.Atdoshin, L.N. Korjavinm Prepr. I.U.P.A.C. Symp. on Macromol. Chem. Prague, 159(1965)
62. A.J.Pennings, internal report (1968)
63. A.J.Pennings, J.M.A.A. van der Mark, J.H. Duysings, internal report (1968)
64. H.Blades, J.R.White, US Patent 3081519 (1963)
65. J.P.Tordella, J. Appl. Phys., 27, 454(1956)
66. A.Ram, "Rheology", Vol.4 F.R. Eyrich, Ed., Academic Press, New York, 251 (1969)
67. J.H.Southerm, D.R.Paul, Pol. Eng. and Sci., 14, 560(1974)
68. J.L.Lebblanc, Rubb. Chem. Technol., 54, 905(1981)
69. W.F.Busse, J. Polym. Sci., A2, 5, 1261(1967)
70. A.S.Krausz, H.Eyring, "Deformation Kinetics", Wiley and Sons, New York, 357(1975)
71. M.Mooney, "Rheology" vol.2., F.Eyrich, Ed. Acad. Press., 181(1958)
72. F.C.Frank, A.Keller, M.R.Mackley, Polymer, 12, 467(1971)
73. R.B.Williamson, W.F.Busse, J. Appl. Phys., 38, 4187(1967)
74. W.George, Appl. Polym. Symp., 27, 159(1975)
75. P.F. van Hutten, A.J.Pennings, to be published
76. J.Smook, P.F. van Hutten, A.J.Pennings, to be published
77. J.L.White, J. Appl. Polym. Sci., Appl. Polym. Symp., 33, 31(1978)
78. G.Marrucci, J.J.Hermans, Macromolecules, 13, 380(1980)
79. K.Yamaura, Y.Go, S. Matsuzawa, "Flow Induced Crystallization of Macromolecules" (in Japanese) (1980); Kolloid Z.u.Z. Polymere, 248, 1030(1971)
80. L.Fischer, R.Haschberger, A.Ziegelendorf, W.Ruland, Coll and Polym. Sci., 260, 174(1980)
81. M.R.Mackley, A.Keller, Phil. Trans. Roy. Soc. London, 278, 29(1975)
82. P.G. de Gennes, "Scaling Concepts in Polymer Physics", Cornell University Press., Ithaca, 119(1979)
83. J.de Boer, A.J.Pennings, Polym. Bull., 5, 317(1981)
84. J.de Boer, A.J.Pennings, Polym. Bull., 7, 309(1982)
85. P.J.Flory, Macromolecules, 12, 119(1979)
86. M.A.Llorente, J.E.Mark, Macromolecules, 13, 681(1980)
87. N.R.Langley, Macromolecules, 1, 348(1968)
88. N.R.Langley, J.D.Ferry, Macromolecules, 1, 353(1968)
89. R.S.Porter, J.F.Johnson, Chem. Rev., 66, 1(1966)
90. D.R.Paul, J.E.St.Laurence, J.H.Fraell, Polym. Eng. and Sci., 10, 70(1970)
91. W.W.Graessley, L.Segal, Macromolecules, 2, 49(1969)
92. J.C.M.Torfs, G.O.R.Alberda van Ekenstein, A.J.Pennings, Eur. Polym. J., 17, 157(1981)
93. S. Gogolewski, A.J.Pennings, J. Appl. Polym. Sci., in press
94. D.S. Boudreaux, J. Polym. Sci., Polym. Phys. Ed., 11, 1285(1973)
95. J.Smook, A.J.Pennings, to be published
96. G.Kanig, Kolloid Z.u.Z. Polymere, 251, 182(1973)
97. A.Peterlin, Fracture, 1, 471(1977)
98. A.Peterlin, J. Macromol. Sci., Phys., B19(3), 401(1981)
99. V.M.Nadkarni, J.M.Schultz, J. Polym. Sci., Phys. Ed., 15, 2151(1979)
100. F.Bueche, J. Chem. Phys., 48, 4781(1968)
101. A.A.Griffith, Phil. Trans. Roy. Soc. Lond., 221, 163(1921)
102. H.H.Kausch, "Polymer Fracture", Springer Verlag Heidelberg (1978)
103. K.E.Porepelkin, Angew. Makromol. Chem., 22, 181(1972)
104. S.N.Zhurkov, V.E.Korsukov, J. Polym. Sci., Polym. Phys. Ed., 12, 385(1974)
105. J.C.M.Torfs, A.J.Pennings, to be published
106. D.C.Prevorsek, Polym. Sci. Symp., 32, 343(1971)
107. E.H.Andrews, P.E.Reed, Advances in Polym. Sci., 27, 1(1978)
108. R.G.Parrish. US Patent 3277221 (1966)